# Spin–orbit interaction in coupled quantum wells*

Hao Ya-Fei(郝亚非)†

*Physics Department, Zhejiang Normal University, Zhejiang* 321004, *China*

(Received 30 May 2012; revised manuscript received 19 July 2012)

We theoretically investigate the spin–orbit interaction in GaAs/$Al_xGa_{1-x}As$ coupled quantum wells. We consider the contribution of the interface-related Rashba term as well as the linear and cubic Dresselhaus terms to the spin splitting. For the coupled quantum wells which bear an inherent structure inversion asymmetry, the same probability density distribution of electrons in the two step quantum wells results in a large spin splitting from the interface term. If the widths of the two step quantum wells are different, the electron probability density in the wider step quantum well is considerably higher than that in the narrower one, resulting in the decrease of the spin splitting from the interface term. The results also show that the spin splitting of the coupled quantum well is not significantly larger than that of a step quantum well.

**Keywords:** spin–orbit interaction, coupled quantum wells, spin splitting

**PACS:** 71.70.Ej, 73.21.Fg, 68.35.bg **DOI:** 10.1088/1674-1056/22/1/017102

## 1. Introduction

Spin degree of freedom has attracted a great deal of interest in theoretical and experimental investigations due to its potential applications in spintronic devices and quantum computing. The electron spin can be electrically controlled in the presence of spin–orbit interaction (SOI).[1] One of the SOIs is the Rashba SOI, which arises from the structure inversion asymmetry (SIA), i.e., the inversion asymmetry of the confining potential in a low-dimensional system.[2] The spin field effect transistor (SFET), which was first proposed by Datta and Das, utilizes the Rashba SOI to control the spin of electrons passing through the SFET.[3] Recently, it has been found that the Rashba SOI can give rise to a pure spin current, which is formed by electrons and holes with the same spin polarization moving along the same direction.[4] An interfacial spin Hall current in a Josephson junction can also be induced by the Rashba SOI.[5] The second SOI is the Dresselhaus SOI, which is due to the inversion asymmetry of semiconductor crystal called the bulk inversion asymmetry (BIA).[6] The interaction between the two kinds of SOIs results in many macroscopic effects.[7,8] If their strengths are the same, the electron spin will not suffer from the DP spin relaxation, resulting in infinite spin relaxation time.[9] Based on the interaction between Rashba and Dresselhaus SOIs, many spintronic devices have been designed.[10,11]

The spintronic devices are usually made up of quantum wells (QWs). Much research has been done on the SOIs of different kinds of QWs, including an asymmetrically doped single QW,[12] single QW with different right and left barriers,[13] asymmetric QW with slope barrier,[14] step QW,[15] and coupled QWs.[16] The coupled QWs are usually realized by sandwiching two single QWs between barriers. We have found that the step QW is more suitable for spintronic devices than a single QW. We wonder whether any new effect will appear in the coupled QWs that are realized by sandwiching two step QWs between barriers. So far, there has been no relevant report about the spin–orbit interaction in such coupled QWs. So we will carry out research on this subject. In this paper, we investigate the spin splitting resulting from the two kinds of SOIs of two different coupled QWs, and explain the origin of the spin splitting resulting from the interface-related Rashba SOI. The results may help to control and manipulate the electron spin via QW structure design.

## 2. Model and method

We consider two different double QWs grown along the [001] direction. We choose axes $X$, $Y$, and $Z$ to be along [100], [010], and [001] directions, respectively. The first double QWs (QWs-I) are realized by sandwiching two GaAs/$Al_{0.3}Ga_{0.7}As$ step QWs between AlAs barriers. The second double QWs (QWs-II) are formed by sandwiching two opposite step QWs (i.e., $Al_{0.3}Ga_{0.7}As$/GaAs and GaAs/$Al_{0.3}Ga_{0.7}As$) between AlAs barriers. The schematic conduction energy band diagrams of QWs-I and QWs-II are shown in the insets of Figs. 1 and 6(a), respectively.

The spin splitting comes from the SIA and the BIA of the QWs. In the absence of an external electric field, if the former and the latter interfaces of an undoped QW cannot transform into each other by a mirror reflection in the well plane, the QW bears an inherent SIA. The Rashba SOI, called the interface-related Rashba SOI in this paper, is localized at the interfaces. The interface term has the form[15] $H_{\rm I} = \alpha_{\rm I}(\sigma_x k_y - \sigma_y k_x)$,

*Project supported by the National Natural Science Foundation of China (Grant No. 61204107) and the Scientific Research Fund of Zhejiang Provincial Education Department, China (Grant No. Y201120799).

†Corresponding author. E-mail: haoyafei@zjnu.cn

© 2013 Chinese Physical Society and IOP Publishing Ltd 

where $k_x$ and $k_y$ are the wave vectors, $\sigma_x$ and $\sigma_y$ denote the spin Pauli matrices, and $\alpha_{\rm I}$ is the interface-related Rashba coefficient. For an abrupt GaAs/$Al_xGa_{1-x}$As interface, $\alpha_{\rm I}$ has the form [15,17] $\alpha_{\rm I} = P\delta(z-z_0)$, where $z_0$ is the position of the interface, and $P$ is the interface parameter, which is related to the difference of band parameters across the interface.[15] The $\delta$ function at $z = z_0$ shows that the Rashba SOI is localized at the interface.[15,17] For the studied structures, each interface contributes to the Rashba SOI, so the interface-related Rashba coefficient can be written as $\alpha_{\rm I} = \sum_i \frac{V_{i\rm L}-V_{i\rm R}}{V_0} P\delta(z-z_i)$, where $z_i$ denotes the $i$-th interface, $V_{i\rm L}$ and $V_{i\rm R}$ are the band edges of the material on the left and the right sides of the $i$-th interface, respectively, and $V_0$ is the band offset of AlAs and GaAs.

The BIA of III and V semiconductor crystal results in the Dresselhaus SOI, which contains linear and cubic Dresselhaus terms. The Dresselhaus SOI terms can be written as[18] $H_{\rm D} = \gamma\langle k_z^2\rangle(\sigma_y k_y - \sigma_x k_x) + \gamma(\sigma_x k_x k_y^2 - \sigma_y k_y k_x^2)$, where $\langle k_z^2\rangle$ is the squared operator $(-{\rm i}\partial/\partial z)$ averaged over the ground state, and $\gamma$ is the cubic Dresselhaus coefficient. So the conduction Hamiltonian can be written as $H = -\frac{\hbar^2}{2m^*}\nabla^2 + V(z) + H_{\rm I} + H_{\rm D}$, where $m^*$ is the electron effective mass, and $V(z)$ is the potential of the double QWs. The Schrödinger equation is solved by using the finite difference method. The present theoretical approach is similar to that in Ref. [19].

## 3. Results and discussion

We numerically calculate the spin splitting resulting from the interface term, and the linear and cubic Dresselhaus terms of the two kinds of double QWs. Obviously, QWs-I is asymmetric in the absence of external and built-in electric fields. The inversion asymmetry (SIA and BIA) can be varied by changing the geometry of the structure. Next, we will show how and why the geometry of QWs-I changes the SIA, the BIA, and the spin splitting.

Figure 1 displays the variations of spin splittings resulting from the interface term and the linear and the cubic Dresselhaus terms each as a function of the width of the central AlAs barrier between two step QWs. The two step QWs are the same, the width of the central barrier is changed. It is observed that the spin splittings resulting from the interface term and the linear Dresselhaus term both increase with the increase of the width of central barrier, reaching maximum values, and then decrease when the width of the central barrier further increases. It has been demonstrated that the spin splitting resulting from the linear Dresselhaus term is related to the confinement of the QW potential, i.e., $\langle k_z^2\rangle$,[12] and the spin splitting resulting from the interface term is related to the electron probability density at each interface of the QW.[15] So the width of the central AlAs barrier changes the spin splitting resulting from the interface term by changing the electron probability density at each interface of the QW.

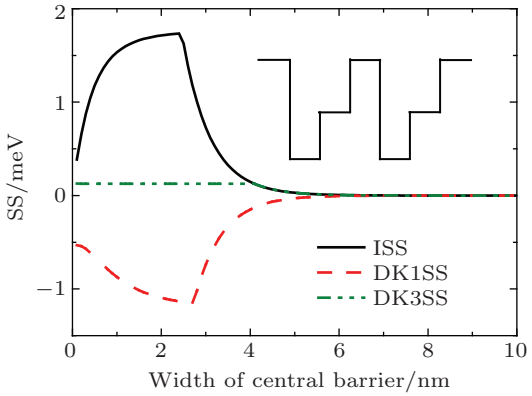



**Fig. 1.** (color online) Variations of spin splittings resulting from the interface term (ISS) and the linear (DK1SS) and the cubic (DK3SS) Dresselhaus terms each as a function of the width of the central AlAs barrier in QWs-I, where the two step QWs are both GaAs/$Al_{0.3}Ga_{0.7}$As step QW. For each step-QW, the width of $Al_{0.3}Ga_{0.7}$As is 3.5 nm, the total width of GaAs and $Al_{0.3}Ga_{0.7}$As is 5 nm. The inset shows the schematic conduction energy band diagram of QWs-I.

We present the electron probability density of QWs-I in Fig. 2. The two step QWs are also the same, the widths of the central barrier are 1 nm, 2 nm, 5 nm, and 7 nm in Figs. 2(a), 2(b), 2(c), and 2(d), respectively. The center of the central barrier is set to be the original point. It is clear from the figures that as the width of the central barrier is narrow, the electron probability densities in the two step QWs overlap, so QWs-I is coupled QWs (CQW-I). When the width of the central barrier is larger than 5 nm, the two step QWs are two independent QWs, and the spin splitting of each step QW is the same as that in Refs. [15] and [20]. By comparing Figs. 2(a) and 2(b), we can find that the maxima of the electron probability densities in the two step QWs are different when the width of the central barrier is 1 nm, and they are nearly the same when the width is 2 nm. So the same probability density distribution of electrons in the coupled two step QWs can result in a large spin splitting from the interface term.

We compare the spin splittings of a step QW and CQW-I in Fig. 3. The width of the central barrier of CQW-I is set to be 1 nm or 2 nm to ensure the two step QWs coupling. The spin splittings of the step QW and the CQW-I with 2-nm-width central barrier have little difference, whereas the spin splittings of the step QW and the CQW-I with 1-nm-width central barrier have obvious differences. This is because the spin splitting of the CQW-I with 1-nm-width central barrier is significantly smaller than that of the CQW-I with 2-nm-width central barrier. So the spin splitting resulting from the three terms in CQW-I is not significantly larger than that of a step QW.

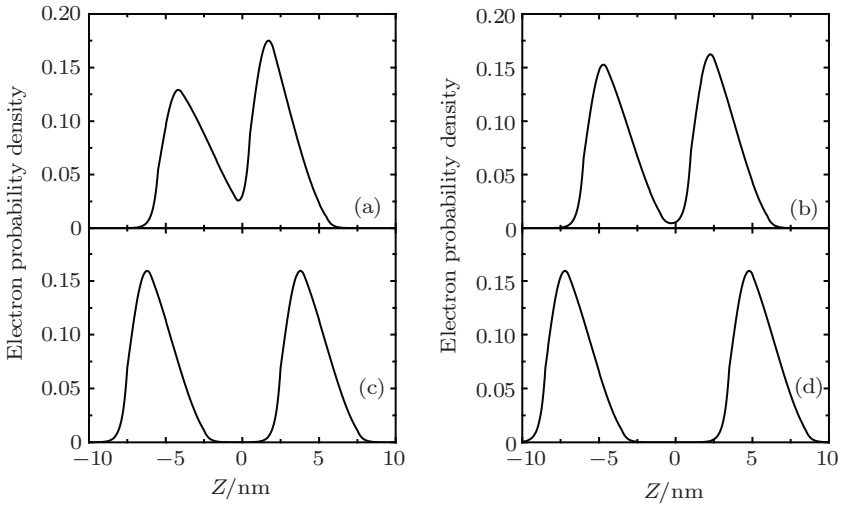



**Fig. 2.** Electron probability densities of QWs-I. The well structure is the same as that in Fig. 1, the widths of central AlAs barrier are (a) 1 nm, (b) 2 nm, (c) 5 nm, and (d) 7 nm respectively.

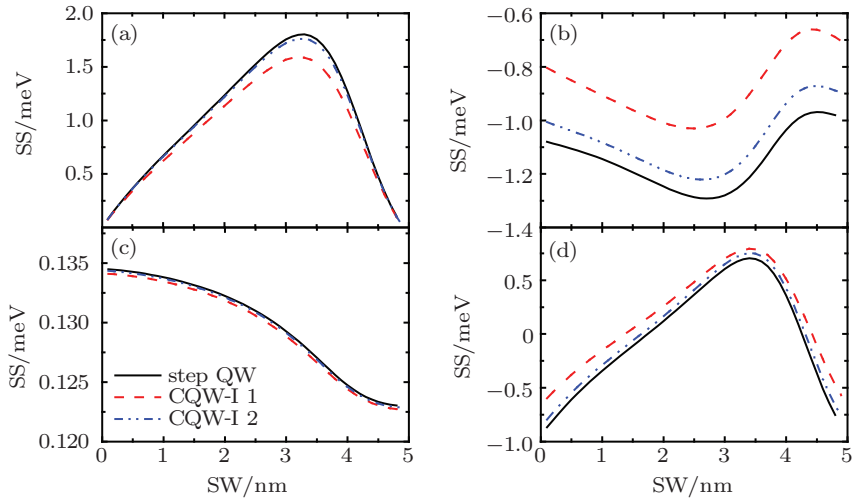



**Fig. 3.** (color online) The spin splittings (SS) resulting from (a) the interface term, (b) the linear and (c) the cubic Dresselhaus terms, as well as (d) the total spin splitting including the contribution of the three terms of a step QW, CQW-I with 1-nm-width central AlAs barrier (CQW-I 1) and CQW-I with 2-nm-width central AlAs barrier (CQW-I 2). The SW denotes the width of $Al_{0.3}Ga_{0.7}As$ step. The total width of GaAs and $Al_{0.3}Ga_{0.7}As$ is 5 nm.

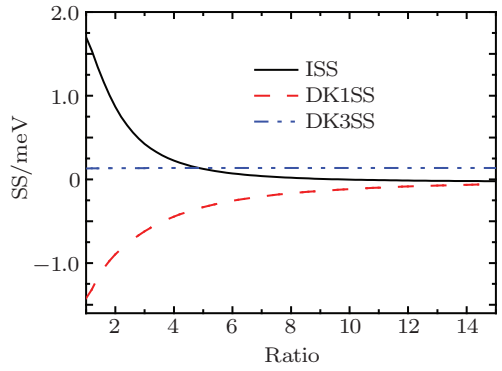



**Fig. 4.** (color online) Variations of spin splittings resulting from the interface term (ISS) and the linear (DK1SS) and the cubic (DK3SS) Dresselhaus terms each as a function of the ratio of the widths of the two step QWs in CQW-I, where the width of the central AlAs barrier is 2 nm, the widths of GaAs and $Al_{0.3}Ga_{0.7}As$ on the left side of the central barrier are both 2 nm, and the widths of GaAs and $Al_{0.3}Ga_{0.7}As$ on the right side of the central barrier are proportional to those on the left side.

For the above CQW-I, the two step QWs are the same. Next, we will show that the spin splitting of CQW-I in which the material is the same but the widths are different. The width of the central barrier is set to be 2 nm. The widths of GaAs and $Al_{0.3}Ga_{0.7}As$ on the left side of the central barrier are both 2 nm, and the widths of GaAs and $Al_{0.3}Ga_{0.7}As$ on the right side of the central barrier are proportional to those on the left side. Figure 4 displays the variations of the spin splittings resulting from the interface term and the linear and the cubic Dresselhaus terms each as a function of the ratio of the widths of the two step QWs. It is clear that the spin splittings resulting from the interface term and the linear Dresselhaus term both decrease with the increase of this ratio.

In order to explain the variation of the spin splitting resulting from the interface term with this ratio, we plot the wave function of CQW-I in Fig. 5. The ratios are 1, 1.5, 2, and 4 in Fig. 5(a), 5(b), 5(c), and 5(d), respectively. The center of the central barrier is set to be the original point. When the ratio is 1, the electron energy level of the ground state

is higher than the potential energy of the $Al_{0.3}Ga_{0.7}As$ conduction band, so the two step QWs are coupled. The wave functions are the same in the two step QWs, showing that the probabilities of electrons appearing in the two step QWs are the same. When the ratio is bigger than 1, the electron energy level of the ground state decreases with the increase of width of the right step QW. The probability of electrons appearing in a wider step QW is higher, so electrons are mainly bound in the wider step QW on the right side of the central barrier. On this occasion, the narrower step QW on the left side of the central barrier makes a small contribution to the spin splitting resulting from the interface term. So the whole CQW-I seems like a wider step QW. The bigger the ratio, the wider the step QW. It is known that the spin splitting resulting from the interface term decreases with the increasing well width.[15] Therefore, it is reasonable that the spin splitting resulting from the interface term decreases with the increasing ratio.

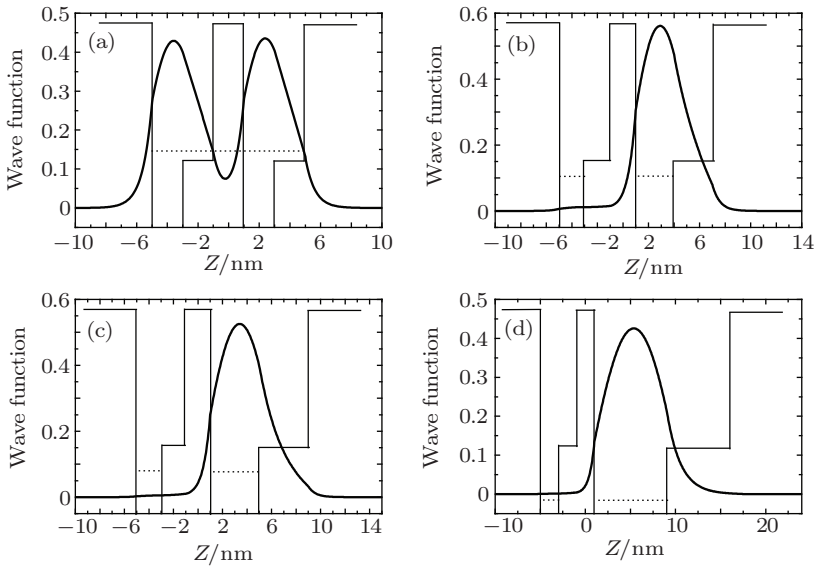



**Fig. 5.** Wave functions of CQW-I, where the width of the central AlAs barrier is 2 nm, the widths of GaAs and $Al_{0.3}Ga_{0.7}As$ on the left side of central barrier are both 2 nm. The widths of GaAs and $Al_{0.3}Ga_{0.7}As$ on the right side of central barrier are (a) 1, (b) 1.5, (c) 2, and (d) 4 times those on the left side. The dashed line denotes the electron energy level of the ground state.

We also calculate the spin splitting of QWs-II, which is a symmetric structure in the absence of external and built-in electric fields. Figure 6(a) shows that the spin splitting resulting from the interface term is zero, which is because the symmetric confinement potential cannot lead to the Rashba SOI. The spin splitting resulting from the linear Dresselhaus term increases to a maximum and then decreases with the increase of the width of the central barrier. When the width of the central barrier is greater than 6 nm, the two step QWs are independent of each other. When it is less than 6 nm, QWs-II is coupled QWs (CQW-II). This can be demonstrated by using the electron probability density in Fig. 6(b). Different from the electron probability density in Fig. 2, in which the electron probability densities are asymmetric, the electron probability densities in Fig. 6(b) are symmetric. Therefore, the results in Fig. 6(b) are in good agreement with the spin splitting resulting from the interface term in Fig. 6(a).

The inversion symmetry of CQW-II can be broken through a structure design. We point out two methods. (i) If the well widths of the two step QWs are different, CQW-II bears an inherent SIA in the absence of external and built-in electric fields. The spin splitting resulting from the interface term is nonzero, and decreases with the increase of the ratio of the widths of the two step QWs, as shown in Fig. 6(c). (ii) The SIA can also be introduced by changing the Al concentration in $Al_{0.3}Ga_{0.7}As/Al_xGa_{1-x}As$ step QW on the left side of the central barrier. The Al concentration is varied from 0 to 0.3, the spin splitting resulting from the interface term increases from 0 meV to 1.5 meV.

In the above figures, it seems that the spin splitting resulting from the cubic Dresselhaus term does not change with the width of the central barrier, the ratio of the widths of the two step QWs, or the Al concentration. In fact, the spin splitting resulting from the cubic Dresselhaus term is not a constant. Compared with the spin splittings resulting from the interface term and the linear Dresselhaus term, it varies little with the alternating quantities. The spin splitting resulting from the cubic Dresselhaus term is proportional to Dresselhaus SOI coefficient $|\gamma|$, which falls with confinement energy $E_{1e}$.[21] In Fig. 7, we plot the spin splitting resulting from the cubic Dresselhaus term as a function of $E_{1e}$. Apparently, the spin splitting resulting from the cubic Dresselhaus term decreases with the increase of $E_{1e}$. This result is in good agreement with experimental results.[21]

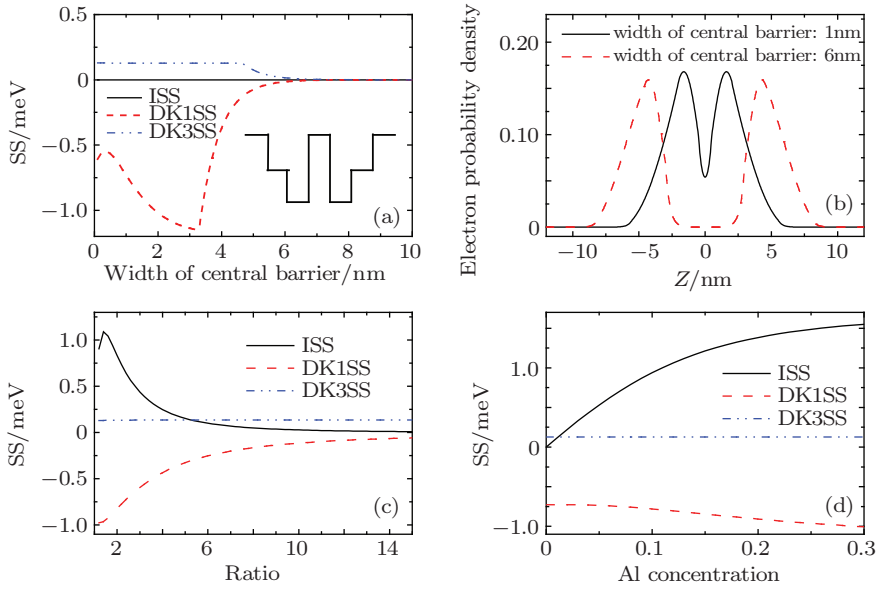



**Fig. 6.** (color online) (a) Variations of spin splittings resulting from the interface term (ISS) and the linear (DK1SS) and the cubic (DK3SS) Dresselhaus terms each as a function of the width of the central AlAs barrier in QWs-II, where the two step QWs are $Al_{0.3}Ga_{0.7}As/GaAs$ step QW and $GaAs/Al_{0.3}Ga_{0.7}As$ step QW. For each step QW, the width of $Al_{0.3}Ga_{0.7}As$ is 3.5 nm, the total width of GaAs and $Al_{0.3}Ga_{0.7}As$ is 5 nm. (b) Electron probability densities of QWs-II. (c) Variations of spin splittings resulting from the interface term (ISS) and the linear (DK1SS) and the cubic (DK3SS) Dresselhaus terms each as a function of the ratio of the widths of the two step QWs in CQW-II, where the width of central AlAs barrier is 1 nm, the widths of GaAs and $Al_{0.3}Ga_{0.7}As$ on the left side of central barrier are 1.5 nm and 3.5 nm, respectively. The widths of GaAs and $Al_{0.3}Ga_{0.7}As$ on the right side of central barrier are proportional to those on the left side. (d) Variations of spin splittings resulting from the interface term (ISS) and the linear (DK1SS) and the cubic (DK3SS) Dresselhaus terms each as a function of Al concentration $x$ on the left $Al_{0.3}Ga_{0.7}As/Al_xGa_{1-x}As$ step QW. The inset in panel (a) shows the schematic conduction energy band diagram of QWs-II.

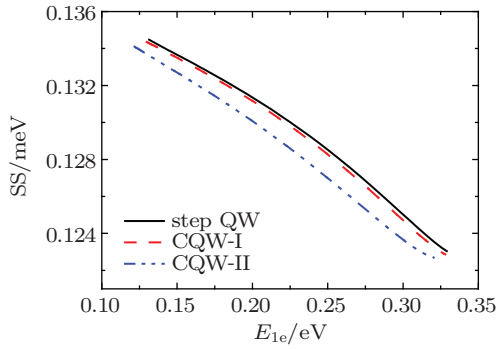



**Fig. 7.** (color online) The spin splitting (SS) resulting from the cubic Dresselhaus term as a function of electron confinement energy $E_{1e}$ for the step QW, CQW-I, and CQW-II.

## 4. Conclusion

We theoretically investigate the spin splittings of two different double QWs. The first bears an inherent SIA in the absence of external and built-in electric fields. When the width of the central barrier is less than 5 nm, the double QWs are CQW-I, and a suitable width of the central barrier results in a large spin splitting resulting from the interface term. The large spin splitting can be attributed to the same probability density distribution of electrons in the two step QWs of CQW-I in which the two step QWs are the same. If the material of the two step QWs is the same but the widths of them are different, the electrons are mainly bound in the wider one of the two step QWs, resulting in the decrease of the spin splitting from the interface term. The second double QWs have a symmetric structure in the absence of external and built-in electric fields. The structure inversion symmetry can be broken by changing its geometry or by changing the Al concentration. We hope the results may be useful for the design of spintronic devices.

## References


[1] Stanescu T D and Galitski V 2007 *Phys. Rev.* B **75** 125307
[2] Bychkov Yu A and Rashba E I 1984 *J. Phys.* C: *Solid State Phys.* **17** 6039
[3] Datta S and Das B 1989 *Appl. Phys. Lett.* **56** 665
[4] Ye C Z, Nie Y H and Liang J Q 2011 *Chin. Phys.* B **20** 127202
[5] Yang Z H, Yang Y H and Wang J 2012 *Chin. Phys.* B **21** 057402
[6] Dresselhaus G 1955 *Phys. Rev.* **100** 580
[7] Wu M W, Jiang J H and Weng M Q 2010 *Physics Reports* **493** 61
[8] Song H Z, Zhang P, Duan S Q and Zhou X G 2006 *Chin. Phys.* B **15** 3019
[9] Averkiev N S, Golub L E and Willander M 2002 *J. Phys.*: *Condens. Matter* **14** R271
[10] Schliemann J, Carlos Egues J and Loss D 2003 *Phys. Rev. Lett.* **90** 146801
[11] Hall K C, Lau W H, Gündoğdu K, Flatté M E and Boggess T F 2003 *Appl. Phys. Lett.* **83** 2937
[12] Koralek J D, Weber C P, Orenstein J, Bernevig B A, Zhang S C, Mack S and Awschalom D D 2009 *Nature* **458** 610
[13] de Andrada e Silva E A, La Rocca G C and Bassani F 1997 *Phys. Rev.* B **55** 16293
[14] Averkiev N S, Golub L E, Gurevich A S, Evtikhiev V P, Kochereshko V P, Platonov A V, Shkolnik A S and Efimov Yu P 2006 *Phys. Rev.* B **74** 033305
[15] Hao Y F, Chen Y H, Liu Y and Wang Z G 2009 *Europhys. Lett.* **85** 37003
[16] Larionov A V and Golub L E 2008 *Phys. Rev.* B **78** 033302
[17] Pfeffer P and Zawadzki W 1999 *Phys. Rev.* B **59** R5312
[18] Winkler R 2004 *Phys. Rev.* B **69** 045317
[19] Hao Y F, Chen Y H, Hao G D and Wang Z G 2009 *Chin. Phys. Lett.* **26** 37103
[20] Hao Y F 2010 *Physica* E **43** 639
[21] Leyland W J H, Harley R T, Henini M, Shields A J, Farrer I and Ritchie D A 2007 *Phys. Rev.* B **76** 195305